PHYSICAL REVIEW LETTERS

Strong Coupling between Localized Plasmons and Organic Excitons in Metal Nanovoids

Y. Sugawara, T. A. Kelf, and J. J. Baumberg

School of Physics and Astronomy, University of Southampton, Highfield, Southampton, SO17 1BJ, United Kingdom

M. E Abdelsalam and P. N. Bartlett

School of Chemistry, University of Southampton, Highfield, Southampton, SO17 1BJ, United Kingdom
(Received 14 June 2006; published 29 December 2006)

Hybrid emitting exciton-plasmonic composites are constructed by coating arrays of spherical nanovoids embedded in a gold film with organic semiconducting molecular *J*-aggregate films. In such plasmonic crystals, localized plasmons confined inside the voids can be excited. We report the first observation of polaritonic spectral narrowing and strong coupling between localized plasmons and *J*-aggregate excitons with Rabi splittings of 230 meV at room temperature.

A key concept in physics is the formation of new quasiparticles from admixtures of strongly-coupled states. Such mixed states can have unusual properties possessed by neither original particle. In the context of light-matter coupling, the interactions between electronic transitions and photonic or plasmonic modes have recently become of interest because their mixed "polariton" states show new optical and electronic properties.[1–5] The polariton modes produced from linear combinations of exciton and localized electromagnetic field experience radically new interactions due to the new dispersion relations formed and the nonlinear optical interactions that take place on them.[5] Most such work has focussed on confining photons in microcavities containing inorganic semiconductors, which however do not strongly couple at room temperature. A particularly promising system of heterostructured hybrid materials that form room-temperature polariton states consists of plasmonic substrates with organic excitons because the plasmons have enhanced optical fields with an almost entirely linear response, while excitons can be electrically-pumped.

Localized plasmons are of interest because strong enhancement and spatial confinement of the electromagnetic field by localized plasmons plays an important role in surface-enhanced Raman spectroscopy [6,7], surface-enhanced fluorescence [8,9], and nano-optical devices [10]. In our work, we use spherical voids to produce localized plasmons, which can be easily tuned by changing the size or the shape of the voids or filling them with a medium. In the study of plasmonic crystals, however, little attention has been paid to the interactions between localized plasmon modes and other delocalized electronic and excitonic states.

Here, we present hybrid plasmonic composites made of metal nanovoids coated with an optically-active molecular excitonic film, and we report the first observation of strong coupling between localized Mie plasmons and *J*-aggregate excitons. Such *J*-aggregates of cyanine dyes, self-organized organic molecular crystals, have partially delocalized excitons with narrow and redshifted absorption bands from that of the dye monomer. Their strong fluorescence is widely investigated for photosensitizer [11] and dye-sensitized solar cell [12] applications. The combination of plasmonic materials and *J*-aggregates is thus a target for functionalized hybrid materials because the narrow line width of *J*-aggregate excitons offers strong coherent interactions with plasmonic modes [13,14]. In addition, the plasmon-enhanced dye fluorescence and high external coupling efficiency of fluorescence trapped inside the luminescent layer enable novel organic light emitters [15] and plasmonic lasers [16].

Recently, we have developed a new type of 2D plasmonic crystal which consists of arrays of spherical metal nanovoids [17,18,20], on which we have observed not only propagating surface plasmon polaritons but also localized plasmons and their mixed modes. The surface plasmon polaritons, which are plasmonic-crystal-like modes, are excited at the Bragg diffraction conditions satisfied between the wave vector of incident light and the periodicity of the plasmonic crystals. The localized plasmon polaritons are excited inside the spherical voids and obey a Mie continuity equation producing generalized "whispering gallery" electromagnetic excitations in the voids. Hence in this Letter, we refer to the two types of plasmons as Bragg plasmons and Mie plasmons, respectively.

Our samples are spherical nanovoid arrays of nanostructured gold covered with an organic dye (chemical structure [21] shown in Fig. 1), which forms a *J*-aggregate. The nanostructured gold is formed using a casting process by electrochemical deposition through a template of self-assembled latex spheres (diameter $d = 600$ nm).[17,18] The resulting metallic mesh reflects the order of the self-assembled template, allowing convenient control of the pore diameters and regularity of the array. Furthermore, by systematically retracting the sample from the plating bath during growth, the nanostructure geometry can be graded. This allows the production of shallow well-spaced
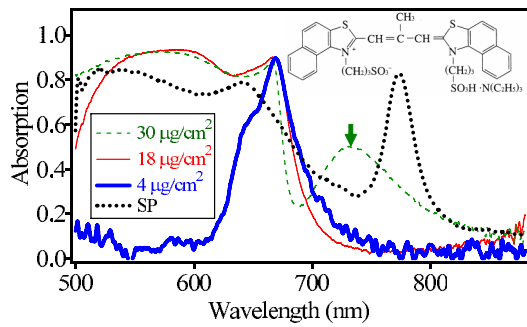
FIG. 1 (color online). Absorption spectra of molecular films formed on flat gold with surface concentrations of 4, 18, and 30 μg/cm^2. Also shown (dashed line) is a typical nonresonant plasmon absorption and (inset) chemical structure of the dye.

FIG. 2 (color online). (a,d) Electron micrographs (SEM) tilted by 45° of the plasmonic crystals with void diameter 600 nm (without a J-aggregate film) at two different thicknesses (a) $t = 170$ nm ($\bar{t} = 0.29$) and (d) $t = 600$ nm ($\bar{t} = 1.00$). (b,c,e,f) Angle-resolved optical reflectivity at $\phi = 0°$ (from 90% to 10%) of the plasmonic crystal of thicknesses $t = 170$ nm (b) without and (c) with a J-aggregate film, and $t = 600$ nm (e) without and (f) with a J-aggregate film.

dishes as well as encapsulated spherical voids on a single sample.

J-aggregated dye films are formed by drop casting a dilute dye solution in methanol onto the gold nanostructured substrate. The thickness and optical properties can be easily controlled by changing dye concentrations. Typical absorption spectra on flat gold substrates [Fig. 1] reveal the narrow exciton absorption band at $\lambda = 670$ nm ($E = 1.85$ eV) for low monomer concentrations. For thicker films from higher surface concentrations (> 10 μg/cm^2), extra peaks of broad monomer absorption around $\lambda = 570$ nm ($E = 2.16$ eV) are also seen because of incomplete J-aggregation. An optical interference mode appears (arrow) when the thickness is similar to the wavelength of light inside the dye film, and which can be used to calibrate the thickness of the J-aggregated films. We find the resulting J-aggregate films to be stable for weeks, with no bleaching effects.

To evaluate plasmonic properties, the reflectivity is angularly-resolved in both incident light angle, θ, and sample orientation, ϕ, over a broad spectral range at different nanovoid thicknesses across each sample. The experiment uses an automated goniometer with a supercontinuum white light laser (wavelengths 480 nm-2 μm) described elsewhere.[17] The spatial-, spectral-, and angular-mapping clearly reveal plasmonic band structures and distinguish plasmonic, photonic, and electronic modes.

First, we focus on two plasmonic crystals of different void thicknesses where almost pure Bragg and Mie plasmons can be observed. Figures 2(a) and 2(d) show SEM images of uncoated plasmonic crystals of two different thicknesses, $t = 170$ nm and 600 nm, corresponding to normalized thickness $\bar{t} = t/d = 0.29$ and 1.00, respectively.

The angle-dependent reflectivity spectra [Fig. 2(b)] for TM-polarized light at an azimuthal angle $\phi = 0°$ (along Γ-K) of the thin ($\bar{t} = 0.29$) plasmonic crystal map of the plasmon-light coupling. For these shallow dished, propagating Bragg plasmons are dominantly present on the top surface of the periodic structure. The observed Bragg plasmons match well to theory (black lines) based on
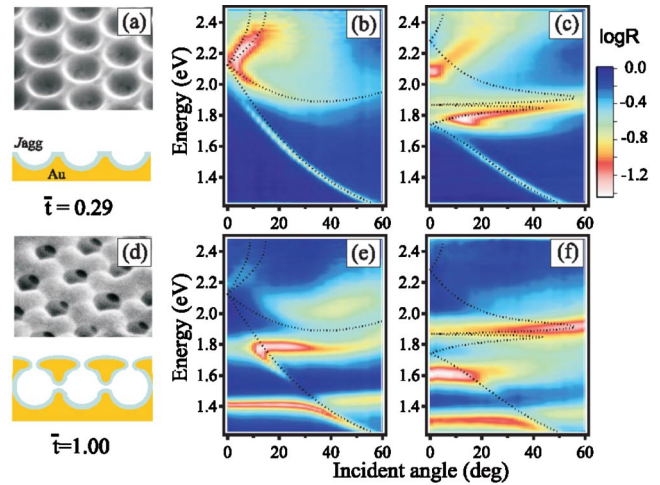
zone-folding the dispersion of surface plasmon polaritons on flat gold. When the plasmonic surface is coated with a 20 nm-thick J-aggregate film, an extra molecular exciton mode appears at 1.85 eV [Fig. 2(c)]. The excitons strongly couple with the Bragg plasmons, splitting the upper and lower bands and producing an anticrossing. The black lines show a theoretical calculation for plasmons propagating along the interface between gold and J-aggregate using dielectric functions built from a single exciton oscillator model fit to the measured absorption in Fig. 1. This theory agrees well for the lower bands, but underestimates the refractive index for energies above the exciton, probably arising from residual monomer contributions. Similar strong coupling has been seen for prism-coupling to propagating surface plasmon polaritons on flat gold coated with J-aggregates[14]. The small ~100 meV "Rabi" coupling strength observed here for the Bragg plasmons is due to the spatial localization of the standing-wave Bloch plasmon mode near $k = 0$ on the flat top surface in between the voids, which partially leaks into the air over the voids outside the J-aggregate layer.

In contrast to the Bragg plasmons, the Mie plasmons for the bare gold voids at $\bar{t} \sim 1$ [Fig. 2(e)] are localized in individual voids and thus have no angular dependence [17]. Both $l = 1$ and $l = 2$ localized plasmons with angular momentum index l are observed at $E = 1.42$ eV and $E = 1.78$ eV, which couple with a Bragg mode on the top surface around 35° and 15°, respectively, showing weak anticrossings. Interaction of the Mie plasmons with the excitons is seen when the J-aggregate film is deposited on this structure [Fig. 2(f)], with the $l = 1$ Mie mode dropping to $E = 1.62$ eV due to the increased refractive

index, and the $l = 2$ Mie mode strongly coupling with excitons to generate two new states repelled in energy.

The strong coupling between J-aggregate excitons and Mie plasmons can be more clearly observed in the dependence of the optical absorption spectra on the void thickness, and hence geometry. Truncating a spherical void raises the energy of the Mie plasmons [17,18], smoothly transforming them into 2D plasmons on the flat surface via shallow dishes at small void thickness. Although Mie plasmon energies in truncated voids cannot yet be calculated, we clearly observe this smooth transformation in Fig. 3(a) into the $l = 2$ mode in the spherical void at $\bar{t} = 1$ (motivating our labelling of these modes as Mie plasmons even for incomplete encapsulation). To lowest order, the Mie mode energies scale inversely with the refractive index of the medium inside the voids [21]; hence, we expect a redshift of the plasmons on coating with the layer of organic semiconductor [solid line, Fig. 3(c)]. After the J-aggregate film is deposited onto the structure, the thickness-dependent dispersion of the Mie mode exhibits a clear anticrossing with the J-aggregate exciton, producing equally admixed states at $\bar{t} = 0.8$. Extracting the energy positions of the reflection dips [Fig. 3(c)] reveals a large polariton Rabi splitting of 230 meV which reflects the strength of overlap of the Mie mode with the J-aggregate inside the void.

This region of strong coupling is examined more closely in Figs. 4(a)–4(c) showing the experimental dispersion for TM-polarized incident light at $\phi = 0°$, $\bar{t} = 0.64$, 0.76, and 0.92, compared to the exciton energy (dashed line). Here again, anticrossing between the J-aggregate excitons (ψ_X) and Mie-like localized plasmons (ψ_{LP}) is clearly observed (arrows). For the situation at $\bar{t} = 0.76$, the exciton-plasmon

polaritons are described by $\psi = \frac{1}{\sqrt{2}}\{\psi_{LP} \pm \psi_X\}$ displaying half-plasmon, half-exciton character localized in each void. Thus the excitons, thought normally to be delocalized over a few nm (tens of molecules) in such J-aggregates, are now combined coherently into wave functions which are delocalized over the void surface, but are not propagating as in previous work. Such plasmon-exciton states are unusual because they mix single-particle excitons (bound electron-hole pairs) with multiparticle excitations (collective electron oscillations) in a solid.

Another feature of this mixing process is that the linewidth of the mixed polaritons is narrower than either of the composite particles. This has been previously ascribed to the induced delocalization averaging over more of the disorder in the sample[22]. The linewidth of the localized plasmon is governed by both radiative and absorptive damping with an inhomogeneous component arising from the 2% disorder in the size of the spheres used for templating. The linewidth of the excitons is controlled by different local configurations of the molecular orientation which change the molecular coupling, as well as radiative damping and dephasing. These contributions alter as the void thickness is increased due to modifications in coupling to the external photon density of states, and the different J-aggregate configuration. Examining the linewidth of the polaritons as a function of the thickness [Fig. 3(e)] reveals polaritonic spectral narrowing around the strong coupling condition. This implies significant contribution to the bare linewidth from molecular excitonic inhomogeneities in the samples.

Because the Mie plasmons are localized, their energy is normally not affected by the orientation of their excitation within the plane. Hence, cuts of the dispersion map $R(\omega, k_x, k_y)$ at a particular energy [Fig. 4(i)] appear circular
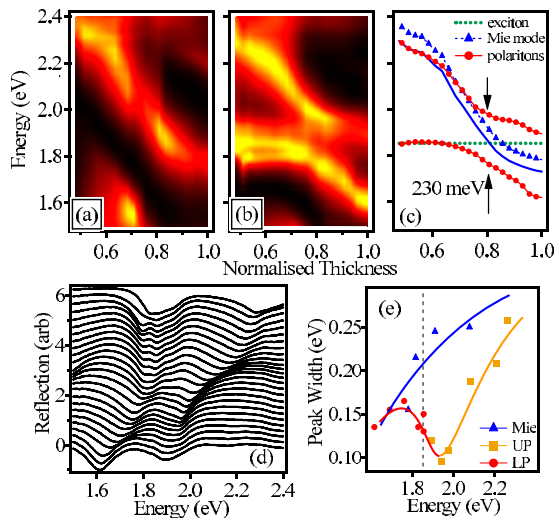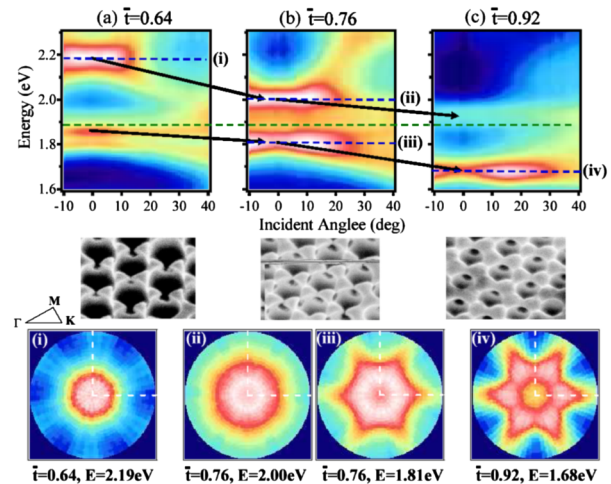

FIG. 3 (color online).   Normal incidence reflectivity vs. void thickness (a) without and (b,d) with the 20 nm J-aggregate film. (c) Extracted reflectivity dip energies with ($\bullet$) and without ($\blacktriangle$) J-aggregate band (exciton dotted line). (e) Extracted absorption linewidths (FWHM) vs mode energy for upper (UP) and lower (LP) polaritons.

FIG. 4 (color online).   Angle-resolved reflectivity spectra for TM-polarized incident light at $\phi = 0°$ for increasing void thickness, $\bar{t}$ (a–c), with exciton band indicated (dashed line), and corresponding SEM images for each thickness. (i–iv) Dispersion in the θ (radial)—ϕ (azimuthal) plane at specific energies labeled.
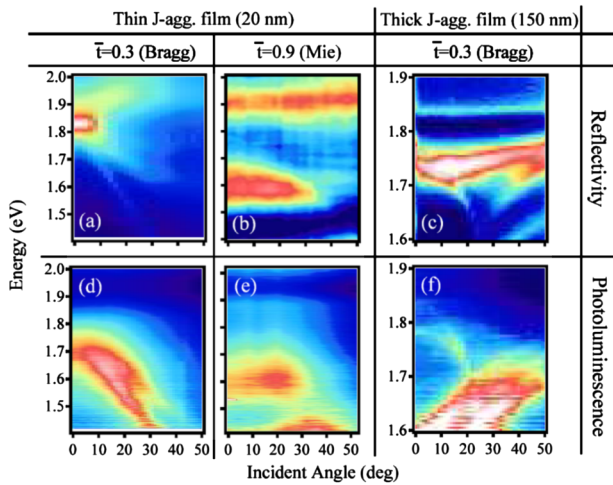
FIG. 5 (color online). Angle-resolved reflection and photoluminescence (PL) spectra for Bragg modes on thin dishes ($\bar{t} = 0.3$) with thin [20 nm: (a,d)] and thick [150 nm: (c,f)] J-agg layers, and Mie modes ($\bar{t} = 0.9$) on thin J-agg [20 nm: (b,e)] plasmonic crystals. PL is normalized to that from J-agg layers on flat Au.

with in-plane wave vector direction. However, the close-packed form of our structure produces holes between neighboring voids [Fig. 4], which allow weak intervoid interactions [23]. Thus the localized plasmon in the encapsulated voids shows evidence of preferential coupling into neighboring void directions [Fig. 4(iv)]. In the strong coupling region, we see evidence that upper and lower polaritons couple differently to neighboring voids [Figs. 4(ii) and 4(iii)]; thus, they possess different admixtures of the initially degenerate $l = 2$ d-wave plasmon wave functions, as well as possible admixture of Bragg plasmons. Complete depictions of the coupled wave functions await full calculations of the plasmon states in such truncated spherical voids.

Our hybrid plasmonic crystals show room-temperature excitonic luminescence which is enhanced by the plasmonic coupling. Using 100 W cm^{-2} pump at $\lambda = 532$ nm, we measure the correlation between reflectivity and luminescence enhancement (by normalizing the emission to PL from identical thickness organic layers on flat Au) from both Bragg plasmons [Figs. 5(a) and 5(d)] and Mie plasmon modes [Figs. 5(b) and 5(e)]. We find that the PL enhancement persists to hundreds of meV below the exciton energy, and that the enhancement of the Bragg modes is roughly 10 times more than for the Mie modes. We believe this is due to the greater reabsorption by the localized plasmons and reduced outcoupling for the near-encapsulated configuration [9].

For thicker molecular films on our plasmonic crystals, new modes are present which are trapped within the molecular semiconductor layer. These are observed as the zone-folded bands in Fig. 5(c), which also produce enhanced PL [Fig. 5(f)]. Comparing carefully the dispersion of the enhanced PL shows that it is blue-shifted (by

60 meV) from the strongest plasmon absorption. This further suggests that the balance between plasmon reabsorption and radiative coupling controls which molecules emit PL efficiently [24].

In conclusion, we have fabricated hybrid exciton-plasmonic crystals which consist of gold nanovoids covered with an organic semiconducting film. Absorption spectra clearly show strong coupling between J-aggregate excitons and localized Mie plasmons, forming mixed exciton-plasmon polaritons as the Mie plasmon energies are tuned by the geometry of the structure. Better understanding of such mixed states opens up the potential of engineering exciton-plasmon optical nonlinear devices, plasmonic lasers, organic nanophotonics, and organic electro-luminescent devices.

[1]   D. G. Lidzey *et al.*, Nature (London) **395**, 53 (1998).
[2]   P. A. Hobson *et al.*, Appl. Phys. Lett. **81**, 3519 (2002).
[3]   C. E. Finlayson *et al.*, Appl. Phys. Lett. **86**, 041110 (2005).
[4]   J. R. Tischler, M. S. Bradley, V. Bulovic, J. H. Song, and A. Nurmikko, Phys. Rev. Lett. **95**, 036401 (2005).
[5]   J. J. Baumberg and L. Vina, Semicond. Sci. Technol. **18**, S279 (2003).
[6]   S. Nie and S. R. Emory, Science **275**, 1102 (1997).
[7]   J. J. Baumberg *et al.*, Nano Lett. **5**, 2262 (2005).
[8]   J. Kummerlen, A. Leitner, H. Brunner, F. R. Aussenegg, and A. Wokaun, Mol. Phys. **80**, 1031 (1993).
[9]   J. R. Lakowicz, Anal. Biochem. **337**, 171 (2005).
[10] M. Ohtsu *et al.*, IEEE J. Sel. Top. Quantum Electron. **8**, 839 (2002).
[11] B. Trosken, F. Willig, K. Schwarzburg, A. Ehert, and M. Spitler, J. Phys. Chem. **99**, 5152 (1995).
[12] K. Sayam *et al.*, J. Phys. Chem. B **106**, 1363 (2002).
[13] J. Dintinger, S. Klein, F. Bustos, W. L. Barnes, and T. W. Ebbesen, Phys. Rev. B **71**, 035424 (2005).
[14] J. Bellessa, C. Bonnand, J. C. Plenet, and J. Mugnier, Phys. Rev. Lett. **93**, 036404 (2004).
[15] D. K. Gifford, and D. G. Hall, Appl. Phys. Lett. **81**, 4315 (2002).
[16] T. Okamoto, F. H'Dhili, and S. Kawata, Appl. Phys. Lett. **85**, 3968 (2004).
[17] T. A. Kelf, Y. Sugawara, J. J. Baumberg, M. Abdelsalam, and P. N. Bartlett, Phys. Rev. Lett. **95**, 116802 (2005).
[18] S. Coyle *et al.*, Phys. Rev. Lett. **87**, 176801 (2001).
[19] T. V. Teperik *et al.*, Opt. Express **14**, 1965 (2006).
[20] T. A. Kelf *et al.*, Phys. Rev. B **74**, 245415 (2006).
[21] Dye number NK-2751, Hayashibara Co., Ltd., Tokyo, Japan.
[22] D. M. Whittaker *et al.*, Phys. Rev. Lett. **77**, 4792 (1996).
[23] M. E. Abdelsalam, P. N. Bartlett, J. J. Baumberg, and S. Coyle, Adv. Mater. **16**, 90 (2004).
[24] P. Anger, P. Bharadwaj, and L. Novotny, Phys. Rev. Lett. **96**, 113002 (2006).